Cropland Abandonment and Influencing Factors in Chongqing, China

Han Li [1,2] and Wei Song [1,*]

1   Key Laboratory of Land Surface Pattern and Simulation, Institute of Geographic Sciences and Natural Resources Research, Chinese Academy of Sciences, Beijing 100101, China; lih.19s@igsnrr.ac.cn
2   College of Resources and Environment, University of Chinese Academy of Sciences, Beijing 100049, China
*   Correspondence: songw@igsnrr.ac.cn

Abstract: Cropland abandonment occurs frequently in many countries and regions around the world, particularly in those with poor environmental conditions, such as mountainous regions. In Chongqing county, China, over 76% of the total area is mountainous. Due to the lack of reliable remote sensing monitoring and identification methods, the spatial and temporal distribution of abandoned cropland areas and its underlying causes are poorly understood. Thus, the extent of cropland abandonment in Chongqing, since 2001, was estimated using land use trajectories. The following results were obtained: (1) the cropland abandonment rate was 12.2–15.4% from 2001 to 2020, with an average of 13.3%; (2) hotspots of abandoned cropland were concentrated in the north and southeast. Cropland abandonment was clustered in the northern, southeastern, and southwestern areas; (3) socio-economic factors (including gross domestic product density, population density, and road density) had a greater impact on the spatial distribution of abandoned cropland than environmental factors. Based on the results, the government should strive to reduce production costs associated with poor agricultural infrastructure, sporadic cropland, and higher labor costs by providing grain subsidies, undertaking cropland consolidation, encouraging land transfer, and improving agricultural infrastructure.

Keywords: spatiotemporal distribution; influencing factors; Chongqing; China

1. Introduction

Against the background of accelerated population growth, providing sufficient food for a global population of 9 billion people has become a serious challenge for human society in the 21st century [1,2]. Stable arable land is critical to sustainably provide food for a growing population [3]. Driven by economic globalization, many parts of the world are currently experiencing rapid urbanization, mostly at the expense of cropland. It is expected that, by 2100, 51–63% of new urban land will be derived from arable land, mostly in China, India, and other countries [4]. The contradiction between future cropland reduction and population growth and the resulting food security issues have attracted wide attention and discussion. Especially since 2020, in the context of the COVID-19 pandemic, many countries importing large amounts of grain have been greatly affected and, currently, the grain supply chain is seriously affected. Cultivated land is a rare resource in China, accounting for less than half the global average per capita. China is home to about 19% of the world's population, albeit with limited arable land resources [5]. Under the premise of comprehensively improving the capacity of cropland to continuously increase production, the overall use of abandoned cropland and the improvement of the cropland use rate are approaches to ensure food security.

At present, cropland abandonment is frequent in many countries and regions around the world [6], making it a hot topic in global land use/cover change research [7]. The emergence of abandoned cropland is strongly linked to the transformation of the socio-economic development. Cropland abandonment was first noticed in mountainous areas of Europe at the beginning of the 20th centuries, where it was associated with forest recovery [8]. With the rapid development of the economy, cropland abandonment spread from developed to developing countries, especially in areas with poor geographical conditions (e.g., mountainous areas) [9]. This phenomenon is most common in developed countries including those of Europe, the United States, Australia, and Japan, as well as in mountainous areas of China, South America, and other regions in Southeast Asia [6]. For example, in Chile, 45.1% of the cropland was abandoned between 1985 and 2007 [10], and 20.7 and 13.9% of the croplands in Poland and Ukraine in Europe, respectively, were lost in the 1980s [11]. According to a large-scale survey conducted by Li et al. [12], between 2014 and 2015, the cropland abandonment rate in Chinese mountainous counties was 14.3%.

When extracting the distribution information of abandoned cropland, farmer surveys or remote sensing monitoring methods are often used. For example, Japan conducted a national tracking survey of cropland abandonment, whereas in Europe, annual sample surveys are conducted, with full surveys every 10 years. However, reliable data on cropland abandonment in other countries are scarce [13]. In recent years, remote sensing technology has shown advantages in monitoring spatial and temporal changes in land use and has gradually been applied for the identification of abandoned cropland [14–18]. For this, MODIS (250 m) and Landsat TM (30 m) image data are commonly used to identify abandoned cropland. For example, Alcantara et al. [19] obtained the distribution of arable land in Eastern Europe from 2003 to 2008 using NDVI (Normalized Difference Vegetation Index) time series and phenological information extracted from MODIS data. Similarly, Prishchepov et al. [20] used Landsat TM/ETM+ remote sensing data from 1990 and 2000 to extract abandoned cropland in the European region of post-Soviet Russia. In addition, for Europe, Corine Land Cover was also an important data source due to the small methodological uncertainty. In 2014, Yusoff et al. [21] identified abandoned oil palm areas by a comparison with background historical cropland data based on SPOT-6 and Landsat OLI data. With the continuous development of remote sensing technologies, image resolution has improved to the meter and sub-meter level, providing a better spatial database for the extraction of abandoned cropland. For example, Alonso-Sarría et al. [22] identified abandoned cropland in the Murcia autonomous region of southeastern Spain based on Quick-Bird images and existing land use maps. In previous studies, the extraction of abandoned cropland was recognized based on comparing vegetation changes or land use type transfers. However, the extraction of the abandoned cropland by directly comparing land use changes over a certain period can only determine the land use status during image acquisition, whereas the period of abandonment is difficult to determine due to the lack of continuous land use information. In addition, for some plots that were recently cleared for farming, it is difficult to determine whether they are fallow or abandoned. With the development of aerial remote sensing technologies, aerial photos with a higher resolution are also an important data source for the identification of abandoned cropland. However, one of their disadvantages is the high cost of acquiring images, making it difficult to implement the real-time monitoring of cropland abandonment in large areas.

Cropland abandonment is a dynamic process that is influenced by a range of complex natural and social drivers that change over time and space [23]. It often occurs in low-income agricultural areas, where poor natural conditions affect agricultural profitability [8,24]; such conditions include steep slopes, extreme weather, soil erosion, poor soil conditions, and long distances from settlements [23,25]. Socioeconomic conditions also affect the economic benefits of cropland and are regarded as the major drivers of cropland abandonment. Economic expansion and urbanization promote the development of secondary and tertiary sectors, creating a variety of non-farming jobs. Non-agricultural sectors can provide considerable income opportunities and widen the gap between urban

and rural life, resulting in rural depopulation. In contrast, for many countries in Europe and North America, the share of part-time farms increased significantly, enabling higher income levels. For some countries with low personnel costs, the reduction in the labor force increases the opportunity cost of agriculture, leading to the abandonment of low-quality cropland [26–28].

Identifying cropland abandonment and understanding the influencing factors can help formulate and improve the relevant policies to reduce the negative impacts of cropland abandonment on food security. However, because of the relatively late emergence of cropland abandonment in China, studies on the spatiotemporal patterns and influencing mechanisms are still scarce. In this context, taking Chongqing in China as an example, this paper adapted a monitoring method of cropland abandonment based on annual land use change, tracking and exploring the changes and influencing factors of cropland abandonment from 2001 to 2020. This study contains three main parts: (1) using remote sensing data to reconstruct the land use trajectory of Chongqing and to evaluate the degree of abandoned cropland, (2) revealing the spatial heterogeneity of abandoned cropland, and (3) detecting the factors influencing cropland abandonment based on the two aspects of the natural environment and the social economy.

2. Study Area

Chongqing is located in the southwestern part of China and the subtropical inland area of the Northern Hemisphere, spanning about 5 degrees in longitude and about 4 degrees in latitude (Figure 1). It is situated in the mid-latitude zone, covering an area of 82,400 km^2. There are significant spatial differences in elevation, which ranges from 73.1 to 2796.8 m. The area with an elevation of more than 800 m covers 29,600 km^2, accounting for 37.0% of the total area. Elevation gradually increases from the southwest to the east. Chongqing is often called a mountain city because it is surrounded by numerous hills and low mountains. The climate is a mid-subtropical, humid monsoon climate with hot summers and warm winters. The average temperature of the coldest month (January) is 7.8 °C, and the frost-free period is 340–350 days. The annual average precipitation ranges from 1000 to 1350 mm in most areas. Most of the precipitation is concentrated from May to September, accounting for about 70% of the annual total precipitation. In recent years, with the rapid social and economic development, Chongqing's per capita gross domestic product (GDP) increased from USD 994.6 in 2000 to about USD 12,130.9 in 2020. In 2020, Chongqing's GDP reached USD 388.8 billion, and the three-industry structure ratio is 7.2:40.0:52.8. The grain cultivation area covers nearly 20,030.7 km^2, with an annual grain output of 10.814 million tons. The annual per capita disposable income of the city's residents is USD 4794.6, with USD 6222.8 in urban areas and USD 2544.9 in rural areas. However, the aging society is one of the most prominent issues of Chongqing. According to the data of the seventh population census in 2020, the population groups aged 0–14, 15–59, and over 60 accounted for 15.9%, 62.2%, and 21.9% of the total population, respectively. Chongqing has the second largest population of those aged over 65 in China, with Hechuan and Zhongxian having the largest proportion. The proportion of the labor force is below the national level, whereas the degree of aging is above the national average.
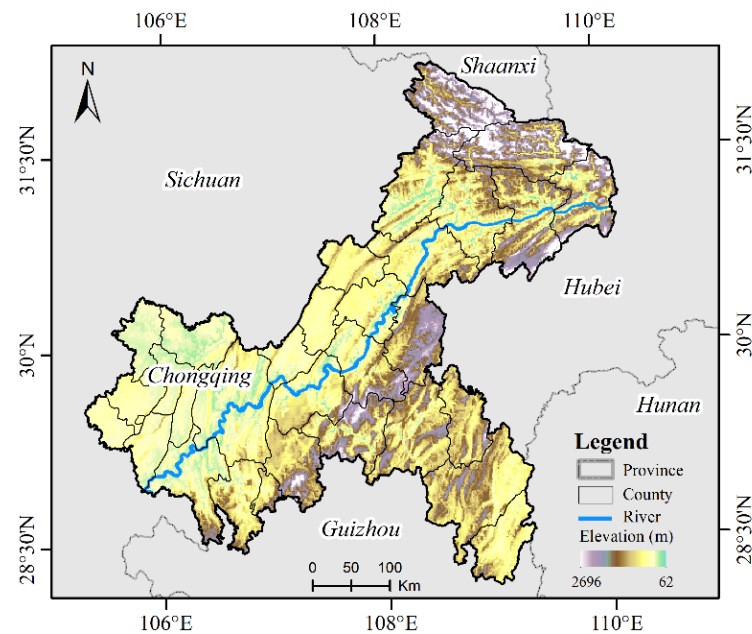
Figure 1. Map showing the geographic Location of Chongqing, China.

3. Materials and Methods

3.1. Data Source

The following three data types were used to extract abandoned cropland (Table 1):

(1) Remote sensing image data. The MODIS Vegetation Index Dataset MOD13Q1 [29] was applied for land use classification of long time series from 2001–2020, including 23 images per year with an actual spatial resolution of about 231 m.

(2) Land use data. To accurately select samples on a large scale, it was necessary to ensure that at least two datasets could be used for intersection each year. The pixels contained in the candidate samples showed the stable land cover types over several years and the high consistency in different land use maps. Four land use data types from different sources were selected to construct a sample database for abandoned cropland training and validation. The first was the MODIS Land Use Product Data MCD12Q1 [29] with the time range from 2001 to 2019 and a spatial resolution of 500 m. The MCD12Q1 data were generated by an integrated decision tree algorithm with an overall accuracy of 75% [30]. The second was the 300-m spatial resolution land use data obtained from the European Space Agency Climate Change Initiative (ESACCI) [31], with a time range of 2001–2019. The overall accuracy for the years 2016, 2017, 2018, and 2019 was estimated at 71.1%, 71.1%, 70.8%, and 70.6%, respectively [31]. The third data type was represented by LUCC data (Land Use and Land Cover) in China with a spatial resolution of 30 m and for the years 2005, 2010, 2015, and 2020. The LUCC data were obtained through remote sensing monitoring based on nationwide field surveys; the overall accuracy exceeded 90% [32]. The data were provided by the Resource and Environmental Science Data Center of the Chinese Academy of Sciences (RESDC) [33]. The fourth data type was GlobeLand30 [34] images with a spatial resolution of 30 m for the year 2020. The overall accuracy of GlobeLand30 in the 2020 data was 85.72%, and the Kappa coefficient was 0.82 [34].

Table 1. Basic data and sources.

Data Category	Type	Time	Source	Resolution	
				Spatial	Temporal
MOD13Q1	Raster	2001–2020	MODIS [29]	250 m	Yearly
MCD12Q1	Raster	2001–2019	MODIS	500 m	Yearly
ESACCI	Raster	2001–2019	European Space Agency [31]	300 m	Yearly
LUCC	Raster	2005, 2010, 2015, 2020	RESDC [33]	30 m	Yearly
GlobeLand30	Raster	2020	National Geomatics Center of China [34]	30 m	Yearly
Elevation	Raster		RESDC	250 m	Yearly
Vegetation type	Raster		RESDC	1 km	Yearly
Soil type	Raster		RESDC	1 km	Yearly
Geomorphological type	Raster		RESDC	1 km	Yearly
Residential distribution	Vector		RESDC	Point	Yearly
Average temperature	Vector	2001–2020	NMSDC [35]	Point	Daily
Precipitation	Vector		NMSDC	Point	Daily
Population	Statistics		Chongqing Statistics Bureau [36]	County	Yearly
Gross domestic product	Statistics		Chongqing Statistics Bureau	County	Yearly
Road length	Statistics		Chongqing Statistics Bureau	County	Yearly

(3) Influencing factors included natural environmental and socio-economical properties, which were used to explore the factors affecting cropland abandonment in the study area. Natural environmental data included elevation, vegetation type, soil type, geomorphological type, residential distribution, temperature, and precipitation. The spatial resolution of elevation was 250 m [33]. Vegetation, soil, and geomorphological types were raster product data extracted from 1:1,000,000-scale Chinese vegetation, soil, and geomorphological maps, respectively, with a spatial resolution of 1 km [33]. The resident distribution was represented by vector point data [33]. Precipitation and temperature were vector meteorological station data provided by the National Meteorological Science Data Center (NMSDC) [35]. The socioeconomic data including county-level statistics, such as population, gross domestic product (GDP), and road length, were derived from the Chongqing Bureau of Statistics [36].

3.2. Definition of Abandoned Cropland

At present, there is no common definition of cropland abandonment. When agricultural activities are ceased, the land is generally considered to be abandoned [6,37,38]. In 1995, the World Food and Agriculture Organization (FAO) defined abandoned cropland as "cultivated land that has not been used for agricultural activities for at least 5 years". In Japan, the Ministry of Agriculture, Forestry, and Fisheries (MAFF) defines it as "land that has not been cultivated for more than 1 year, and there is no indication that it will be cultivated in the following years" [39]. Low et al. [40] defined abandoned cropland as "permanent arable land not managed for at least 4 years". From the length of time taken to abandon an area of cropland, as defined by cropland abandonment, the fallow period is usually at least 2 years. In the China Statistical Yearbook of 2008–2012, the area of cropland includes the cultivated area, leisure land, new land reclamation, and cropland, when abandoned for less than 3 years. Therefore, this paper adopted a time limit of 3 years or more to identify abandoned cropland. We defined abandoned cropland as cropland

that lacks farming management, is potentially characterized by vegetation succession, and where this condition lasts for at least 3 years. Specifically, if the cropland pixels changed to unused land, forest, and grassland, they were marked as suspected, abandoned cropland pixels. If the pixel was marked as a suspected, abandoned cropland pixel for 3 consecutive years, it was defined as an abandoned cropland pixel.

3.3. Research Process

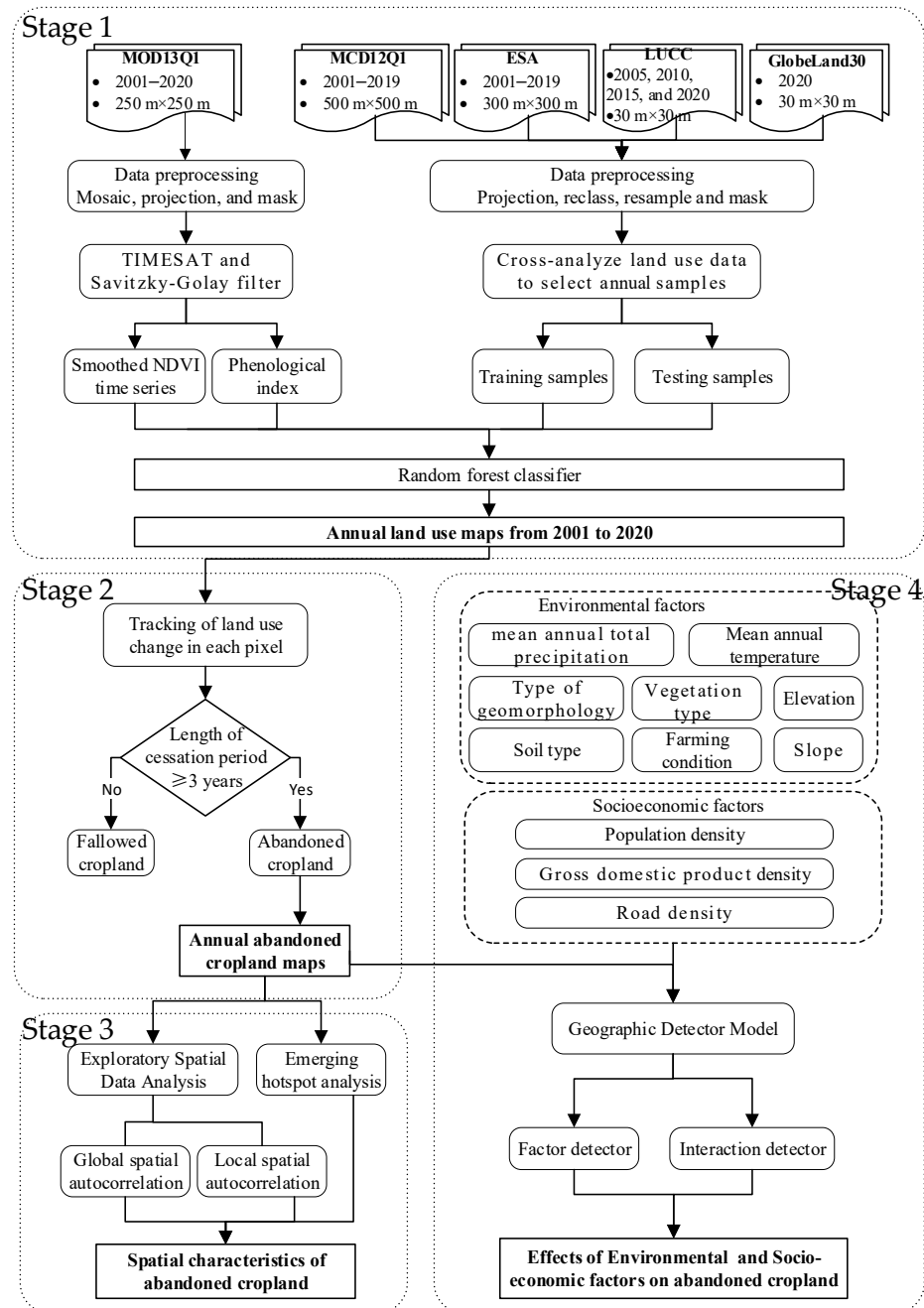The research process adopted here can be divided into the following four stages (Figure 2).

Figure 2. Flow charts showing abandoned cropland patterns and influencing factor analysis process.

Mapping annual land use maps—Stage 1. The data processing part includes the splicing, projection, and clipping of the original data. Subsequently, the Savitzky-Golay filter was used for reconstructing NDVI time series and calculating the annual phenology metrics. Using existing land use data, at least two datasets were crossed each year to select training and validation samples. The smooth NDVI value and annual phenology metrics were entered into the random forest model to classify annual land use for the period 2001–2020. The resolution of the obtained land use data was 250 m.

Extracting the distribution of cropland abandonment—Stage 2. Taking 2001 as the initial state for tracking land use changes, the trajectory of land use change within the cropland boundary since 2001 was detected. Subsequently, the stop farming cycle of each pixel was calculated. Combined with the definition of cropland abandonment, pixels with a stop farming period of 3 years or longer were identified as abandoned cropland, with a spatial resolution of 250 m.

Spatial statistical analysis—Stage 3. Using exploratory spatial data analysis (including global and local spatial autocorrelation) and emerging hotspot analysis, the temporal and spatial distribution changes of abandoned cropland were analyzed on a 5 km grid scale.

Analysis of influencing factors—Stage 4. The effects of natural and socio-economic factors on the spatial distribution of cropland abandonment were studied using a factor and interaction detector on a 5 km grid scale.

3.3.1. Generation of the Annual Land Use Maps

In China, the land use classification of the Ministry of Land and Resources and others based on remote sensing do not delimit abandoned cropland as a separate land type. In addition, there is no accurate definition of abandoned cropland. Although there are some high-resolution land use data, it is difficult to determine the abandonment time of a plot due to the lack of continuous land use information. The method of extracting abandoned cropland, by comparing the changes in land use in a certain interval, may lead to overestimation or underestimation of the abandoned cropland areas. Therefore, we performed a series of processes to produce a continuous long-term series of land use maps. First, the NDVI time series were reconstructed based on the TIMESAT3.3 software to obtain the smoothed NDVI value and the phenological index. Subsequently, reliable training and verification samples were selected. These data were classified as the input data of the random forest classifier. Finally, we obtained the land use maps from 2001 to 2020 with a resolution of 250 m; the specific processing procedures are described in Appendix A.

The selected validation samples were taken as true values to analyze the accuracy of the classified land use in 2001–2020. Based on the confusion matrix tool in the ENVI5.4 software, the overall accuracy and the Kappa coefficient can be calculated. The overall classification accuracy is equal to the total number of correctly classified pixels divided by the total number of pixels. The Kappa coefficient and the overall accuracy can be measured based on the following equations [41]:

$$p_e = \frac{\sum_{i=1}^{m} a_i * b_i}{n^2}, \tag{1}$$

$$k = \frac{p_o - p_e}{1 - p_e}, \tag{2}$$

where "p_o" is the overall classification accuracy, "a_i" is the true sample number of each land use type, "b_i" is the predicted sample number of each land use type, "m" is the total number of land use types, "n" is the total number of samples, and "k" is the Kappa coefficient.

3.3.2. Extracting the Distribution of Cropland Abandonment

The map time stack was constructed using the initial state of the 2001 land use map to obtain the track of each pixel. The annual land type change within the cropland land boundary since 2001 was detected. Combined with the definition of the abandoned cropland, pixels with an abandonment period of 3 years or longer were classified as abandoned cropland. In terms

of the changes in land use type, it takes at least 3 years for cropland to be converted to forest land, grassland, or unused land. Based on the land use trajectory, we calculated the length of the fallow period for each cropland pixel. Finally, we obtained the spatial distribution of cropland abandonment in Chongqing from 2001 to 2020.

3.3.3. Spatial Statistical Analysis

Exploratory spatial data analysis (ESDA, including global and local spatial autocorrelation analysis) was employed to intuitively analyze the spatial clustering characteristics of the abandoned cropland [42]. The purpose of global spatial autocorrelation analysis is to determine whether a variable is spatially correlated and, if so, to what degree [43]. Global Moran's I is often applied to quantitatively describe the spatial dependence of variables [44]. Local spatial autocorrelation describes the similarity between a spatial unit and its domain, which is often reflected by local Moran's I [45]. This index can represent the degree to which each local unit complies with the global general trend. A 5 km grid was produced to calculate the percentage of abandoned cropland in the base year of the 2001 cropland area, and the spatial aggregation characteristics of abandoned cropland were analyzed by using two spatial autocorrelation indices obtained from the ARCGIS 10.2 software.

Emerging hot spot analysis (EHSA) was used to describe the temporal and spatial patterns of abandoned cropland and to analyze its change trend. First, the values of the abandoned cropland rate (% 2001 cropland area) were integrated into a multidimensional dataset using the Space-Time Pattern Mining Toolbox in the ArcGIS software, where each dimension showed the abandoned cropland rate in the 5 km grid squares per year. The Mann–Kendall trend test and Getis-Ord Gi* are the two main statistical indicators of EHSA [46,47]. The former was used to measure the time series trend of a specific location, whereas the latter was applied to determine the distribution of hot and cold clusters of abandoned cropland. According to the two indicators, EHSA can divide the spatiotemporal change results into eight categories, namely historical, oscillating, sporadic, diminishing, persistent, intensifying, consecutive, new hot, and cold spots. A more specific introduction to EHSA can be found in the ArcGIS help documentation [48].

3.3.4. Analysis of Influencing Factors

By comparing the spatial consistency of cropland abandonment and the influencing factors, we explored the main factors influencing cropland abandonment, using factor and interactive detectors of the Geographic Detector Model (GDM). According to Wang and Xu [49], if the spatial distribution of farmland abandonment is similar to that of the selected influencing factor index, the variance within the layer is smaller than that between the layers. The q-statistics were proposed by Wang et al. [49] and applied to assess the determining effect of each influencing factor on the cropland abandonment rate. The value of the q-statistics ranges from 0 to 1; larger values indicate that the influencing factor has a stronger explanatory power for cropland abandonment. The specific calculation method of the q statistics can be found in Appendix A. The interaction detector was used to detect the influence of multi-factor interactions on the explanatory power of the results; the interaction types are shown in Table 2. More information on GDM can be found elsewhere (http://www.geodetector.cn/, accessed on 10 March 2021).

In the influencing factor analysis, the dependent variable was the abandoned cropland rate within the 5 km grid, and the independent variables could be divided into two categories. The first category consisted of natural environmental factors, including digital elevation, slope, geomorphological type (GT), soil type (ST), vegetation type (VT), farming conditions (FC), mean annual total precipitation (MATP), and mean annual temperature (MAT). All data were unified into 5 km spatial resolution data. Based on elevation data, slope was calculated using the slope tool of the ArcGIS10.2 software. The geomorphological types included plain, platform, hills, small, medium- and large-sized mountains; and the soil types included red clay, alluvial, limestone, purplish, skeletal, shajiang black, chao,

paddy, lateritic red earth, red earth, yellow earth, urban area, rock, lake, or reservoir. The vegetation types included coniferous forest, broadleaf forest, shrubs, deserts, steppe, underbrush, cultivated vegetation, and others. The MAT and MATP were generated by interpolation, using the AUSPLINE meteorological interpolation software, based on the daily average temperature and precipitation data of the meteorological stations. The farming conditions, an indicator of difficulty as steep slopes and long commutes generally led to an increase in the values of these variables, were calculated by multiplying the related factors considering the slope of the plot and the farming distance between the plot and the residential area (including horizontal and vertical distance) [50]. The second category was composed of socioeconomic factors, including gross domestic product density (GDPD), population density (PD), and road density (RD). These data were obtained using the Polygon to Raster (Conversion) tool in the ArcGIS10.2 software. Together, these variables could illustrate the social and economic situation of Chongqing.

Table 2. Interaction detector model and interaction types.

Description	Interaction Type
$q (X1 \cap X2) < Min(q (X1), q (X2))$	Non-linear-weakening
$Min(q (X1), q (X2)) < q (X1 \cap X2) < Max(q (X1), q (X2))$	Uni-weakening
$q (X1 \cap X2) > Max(q (X1), q (X2))$	Bi-enhancing
$q (X1 \cap X2) = q (X1) + q (X2)$	Independent
$q (X1 \cap X2) > q (X1) + q (X2)$	Non-linear-enhancing

Note: $q (X1 \cap X2)$ represents the q-statistic value of the interaction effect of factors X1 and X2, and q(X1) and q(X2) represent the effects of X1 and X2, respectively.

4. Results

4.1. Annual Land Use Map

The overall accuracy ranged between 87.5% (in 2014) and 96.7% (in 2006), with an average value of 92.6% (Figure A1). The Kappa coefficient ranged between 0.84 and 0.95, with an average value of 0.90. The land use map from 2001 to 2020 is shown in Figure A2. Despite some variation amongst the years, the overall classification accuracy was high. Figure 3 illustrates the land use change in Chongqing from 2001 to 2020. In the past 20 years, forest, built-up, and water areas increased by 7.2%, 2.6%, and 0.2%, respectively; grassland, cropland, and unused areas decreased by 5.0%, 5.0%, and 0.1%, respectively. From 2001 to 2020, the main feature of the land use spatial change was the conversion of cropland to grassland, forest, and built-up areas, with 7633.26, 2224.13, and 1641.82 km^2 converted, respectively. The expansion of the built-up area mainly occurred at the expense of cropland and grassland, occupying 1641.82 and 589.45 km^2, respectively.
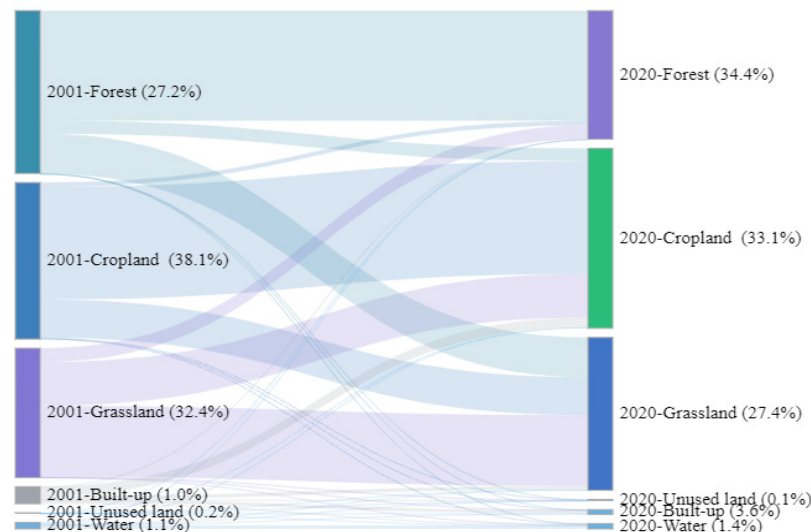
Figure 3. Graph illustrating the conversion of land use types between 2001 and 2020.

4.2. Spatiotemporal Variations in Cropland Abandonment

The abandoned cropland area ranged from 3824.8 to 4824.0 km^2, with an average of 4185.2 km^2 (Figure 4). The cropland abandonment rate was 12.19 to 15.37%, with an average of 13.33%, representing the percentage of abandoned cropland area in 2001. The cropland abandonment rate first increased and then decreased, with the lowest and highest values observed in 2006 and 2013, respectively.
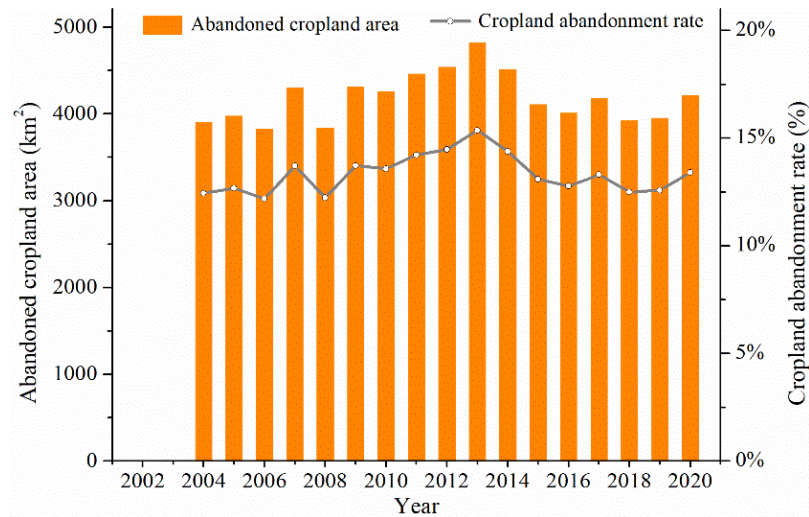
Figure 4. Abandoned cropland area and rate for the period 2001–2020.

We accumulated the cropland abandonment frequency of each pixel from 2001 to 2020 (Figure 5). Since 2001, about 11,576.9 km^2 of farmland was abandoned, accounting for 36.88% of the total area. All counties in Chongqing experienced cropland abandonment. There was a significant spatial difference in the distribution of abandoned cropland areas, with a higher distribution in the north and southeast of Chongqing. In the western regions, abandoned cropland areas were sparse, and cropland was generally only abandoned once. In Jiangjin, Fuling, and Fengdu, the cropland abandonment frequency ranged from once to three times, whereas frequencies higher than twice were found in the following counties: Youyang, Xiushan, Pengshui, Qianjiang, Wanzhou, Zhong, Kai, and Qijiang.
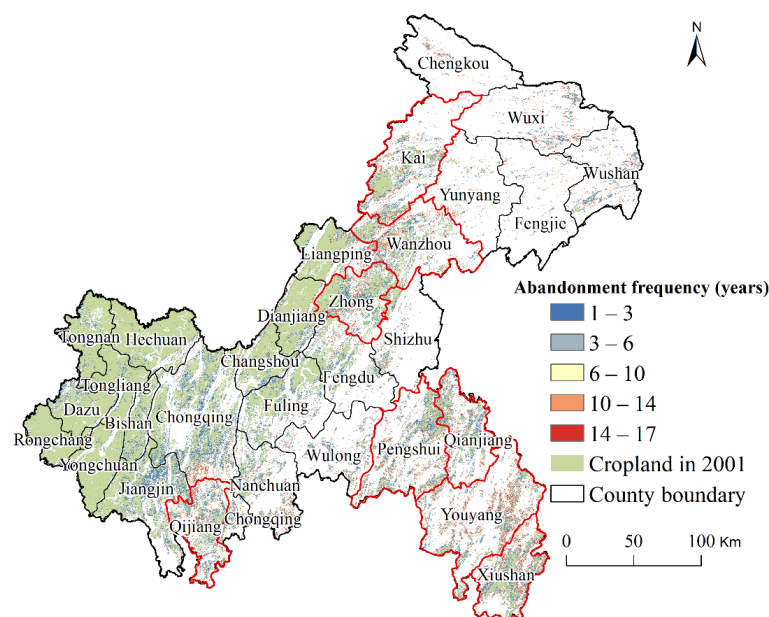
Figure 5. Distribution of cropland abandonment frequency in Chongqing from 2001 to 2020.

From 2001 to 2020, the cropland abandonment rate in most counties of Chongqing showed an increasing trend, whereas, in some areas, such as Chengkou and Wuxi, it increased first and then decreased (Figure 6). The areas with values above the average of the Chongqing average were mainly distributed in the southeast areas, such as Chengkou and Fengjie, whereas regions with lower values were mainly found in the southwest areas, such as Tongliang and Bishan. Among them, Chengkou had the highest average cropland abandonment rate of 47.5%, whereas Rongchang had the lowest rate of 0.6%.

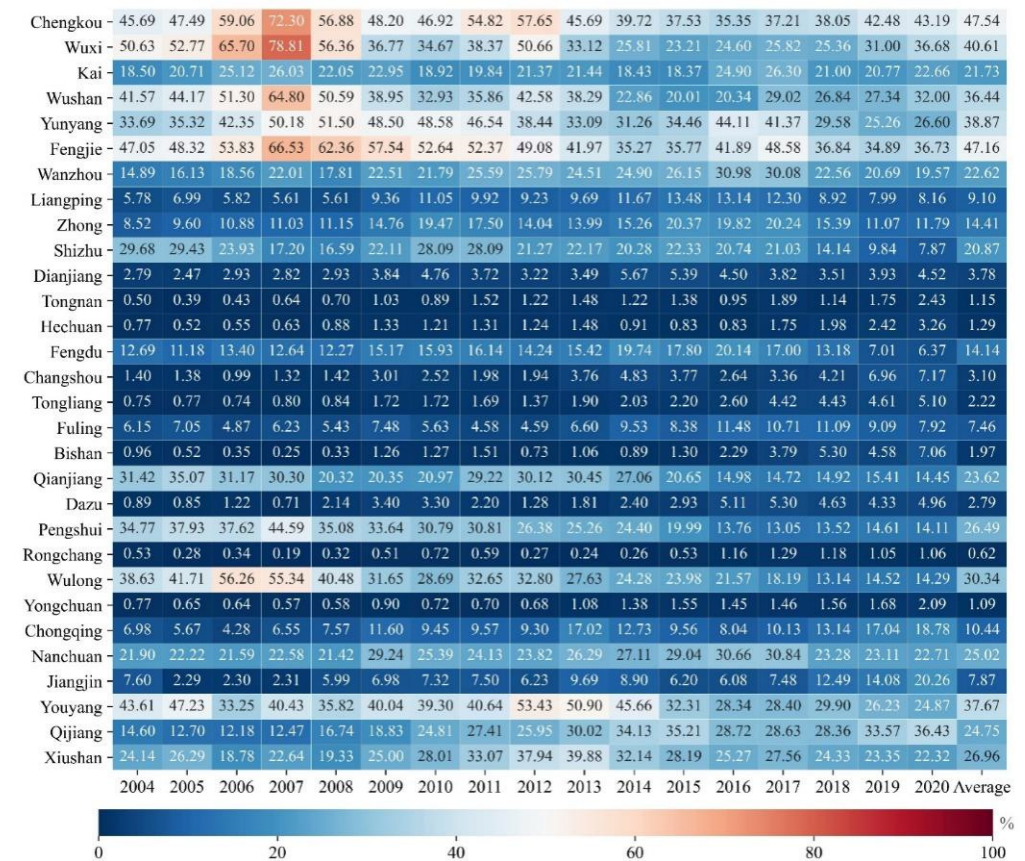| County	2004	2005	2006	2007	2008	2009	2010	2011	2012	2013	2014	2015	2016	2017	2018	2019	2020	Average
Chengkou	45.69	47.49	59.06	72.30	56.88	48.20	46.92	54.82	57.65	45.69	39.72	37.53	35.35	37.21	38.05	42.48	43.19	47.54
Wuxi	50.63	52.77	65.70	78.81	56.36	36.77	34.67	38.37	50.66	33.12	25.81	23.21	24.60	25.82	25.36	31.00	36.68	40.61
Kai	18.50	20.71	25.12	26.03	22.05	22.95	18.92	19.84	21.37	21.44	18.43	18.37	24.90	26.30	21.00	20.77	22.66	21.73
Wushan	41.57	44.17	51.30	64.80	50.59	38.95	32.93	35.86	42.58	38.29	22.86	20.01	20.34	29.02	26.84	27.34	32.00	36.44
Yunyang	33.69	35.32	42.35	50.18	51.50	48.50	48.58	46.54	38.44	33.09	31.26	34.46	44.11	41.37	29.58	25.26	26.60	38.87
Fengjie	47.05	48.32	53.83	66.53	62.36	57.54	52.64	52.37	49.08	41.97	35.27	35.77	41.89	48.58	36.84	34.89	36.73	47.16
Wanzhou	14.89	16.13	18.56	22.01	17.81	22.51	21.79	25.59	25.79	24.51	24.90	26.15	30.98	30.08	22.56	20.69	19.57	22.62
Liangping	5.78	6.99	5.82	5.61	5.61	9.36	11.05	9.92	9.23	9.69	11.67	13.48	13.14	12.30	8.92	7.99	8.16	9.10
Zhong	8.52	9.60	10.88	11.03	11.15	14.76	19.47	17.50	14.04	13.99	15.26	20.37	19.82	20.24	15.39	11.07	11.79	14.41
Shizhu	29.68	29.43	23.93	17.20	16.59	22.11	28.09	28.09	21.27	22.17	20.28	22.33	20.74	21.03	14.14	9.84	7.87	20.87
Dianjiang	2.79	2.47	2.93	2.82	2.93	3.84	4.76	3.72	3.22	3.49	5.67	5.39	4.50	3.82	3.51	3.93	4.52	3.78
Tongnan	0.50	0.39	0.43	0.64	0.70	1.03	0.89	1.52	1.22	1.48	1.22	1.38	0.95	1.89	1.14	1.75	2.43	1.15
Hechuan	0.77	0.52	0.55	0.63	0.88	1.33	1.21	1.31	1.24	1.48	0.91	0.83	0.83	1.75	1.98	2.42	3.26	1.29
Fengdu	12.69	11.18	13.40	12.64	12.27	15.17	15.93	16.14	14.24	15.42	19.74	17.80	20.14	17.00	13.18	7.01	6.37	14.14
Changshou	1.40	1.38	0.99	1.32	1.42	3.01	2.52	1.98	1.94	3.76	4.83	3.77	2.64	3.36	4.21	6.96	7.17	3.10
Tongliang	0.75	0.77	0.74	0.80	0.84	1.72	1.72	1.69	1.37	1.90	2.03	2.20	2.60	4.42	4.43	4.61	5.10	2.22
Fuling	6.15	7.05	4.87	6.23	5.43	7.48	5.63	4.58	4.59	6.60	9.53	8.38	11.48	10.71	11.09	9.09	7.92	7.46
Bishan	0.96	0.52	0.35	0.25	0.33	1.26	1.27	1.51	0.73	1.06	0.89	1.30	2.29	3.79	5.30	4.58	7.06	1.97
Qianjiang	31.42	35.07	31.17	30.30	20.32	20.35	20.97	29.22	30.12	30.45	27.06	20.65	14.98	14.72	14.92	15.41	14.45	23.62
Dazu	0.89	0.85	1.22	0.71	2.14	3.40	3.30	2.20	1.28	1.81	2.40	2.93	5.11	5.30	4.63	4.33	4.96	2.79
Pengshui	34.77	37.93	37.62	44.59	35.08	33.64	30.79	30.81	26.38	25.26	24.40	19.99	13.76	13.05	13.52	14.61	14.11	26.49
Rongchang	0.53	0.28	0.34	0.19	0.32	0.51	0.72	0.59	0.27	0.24	0.26	0.53	1.16	1.29	1.18	1.05	1.06	0.62
Wulong	38.63	41.71	56.26	55.34	40.48	31.65	28.69	32.65	32.80	27.63	24.28	23.98	21.57	18.19	13.14	14.52	14.29	30.34
Yongchuan	0.77	0.65	0.64	0.57	0.58	0.90	0.72	0.70	0.68	1.08	1.38	1.55	1.45	1.46	1.56	1.68	2.09	1.09
Chongqing	6.98	5.67	4.28	6.55	7.57	11.60	9.45	9.57	9.30	17.02	12.73	9.56	8.04	10.13	13.14	17.04	18.78	10.44
Nanchuan	21.90	22.22	21.59	22.58	21.42	29.24	25.39	24.13	23.82	26.29	27.11	29.04	30.66	30.84	23.28	23.11	22.71	25.02
Jiangjin	7.60	2.29	2.30	2.31	5.99	6.98	7.32	7.50	6.23	9.69	8.90	6.20	6.08	7.48	12.49	14.08	20.26	7.87
Youyang	43.61	47.23	33.25	40.43	35.82	40.04	39.30	40.64	53.43	50.90	45.66	32.31	28.34	28.40	29.90	26.23	24.87	37.67
Qijiang	14.60	12.70	12.18	12.47	16.74	18.83	24.81	27.41	25.95	30.02	34.13	35.21	28.72	28.63	28.36	33.57	36.43	24.75
Xiushan	24.14	26.29	18.78	22.64	19.33	25.00	28.01	33.07	37.94	39.88	32.14	28.19	25.27	27.56	24.33	23.35	22.32	26.96

**Figure 6.** Cropland abandonment rates of counties in Chongqing from 2001 to 2020.

4.3. Spatial Statistics of Abandoned Cropland

The cropland abandonment rates for the four subperiods (2001–2005, 2006–2010, 2011–2015, and 2016–2020) were 30.56%, 30.57%, 26.87%, and 22.97%, respectively, with an initial slight increase and a subsequent decrease (Figure A3). The abandonment rates of mountainous counties in the north and southeast of Chongqing were considerably higher than those in the west. The global Moran index of the cropland abandonment rate in the four sub-periods passed the significance test, showing values of 0.661, 0.669, 0.568, and 0.470, respectively (Figure 7). This suggested that the spatial distribution of abandoned cropland was positively correlated with a high degree of clustering. The overall cluster trend increased first and then decreased slightly from 2001 to 2020. The local spatial autocorrelation index values of the four sub-periods showed a similar spatial aggregation distribution. The spatial agglomeration type was dominated by high–high and low–low areas, with a wide range of distribution. The high–high type was mainly distributed in the north and southeast, such as in Chengkou, Wuxi, and Youyang, whereas the low–low areas were mainly distributed in the southwest, such as Tongnan, Hechuan, Tongliang, and Dazu. The distribution range of high–low and low–high areas was smaller than that of the other cluster types. High–high and low–low clustering showed a downward trend; for example, the proportion of high–high areas decreased from 18% in 2001–2005 to 12% in 2016–2020, and the low–low areas decreased from 25 to 14% in the same period.
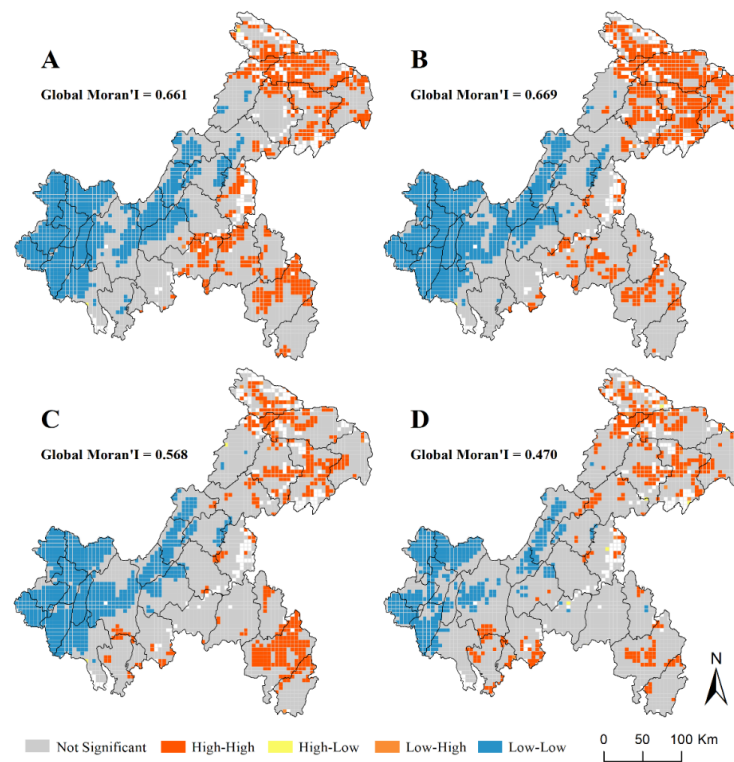
Figure 7. Spatial clustering types within 5 km grid squares in Chongqing (**A**) between 2001 and 2005, (**B**) between 2006 and 2010, (**C**) between 2011 and 2015, and (**D**) between 2016 and 2020.

The results of the EHSA show the temporal and spatial patterns of cropland abandonment from 2001 to 2020 (Figure 8). Oscillating, diminishing, sporadic, and persistent cold spots were the dominant evolutionary patterns of abandoned cropland. The diminishing cold spots were concentrated in the west, such as in Hechuan and Tongliang County, whereas the sporadic cold spots were concentrated in central Chongqing, such as Fengdu County; persistent cold spots were concentrated in the west, such as in Hechuan, Tongnan, and Rongchang County. In general, the abandoned cropland from the past 20 years was dominated by cold spots.
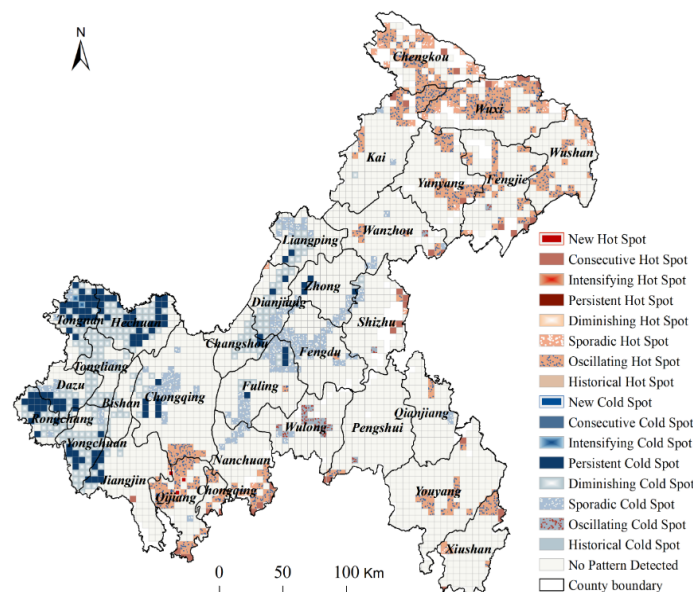
Figure 8. Cropland abandonment EHSA (emerging hot spot analysis) results for the period between 2001 and 2020.

4.4. Determinants and Interactions of Cropland Abandonment

In this study, the GDM method was used to identify the determinants and interaction effects of cropland abandonment in Chongqing. The dependent variables were the cropland abandonment rates in 2005, 2010, 2015, 2020, and for the entire period of 2001–2020, and the independent variables were the socio-economic and environmental factors. Based on the factor detector in GDM, the q-statistics representing the explanatory power of each independent variable for abandoned cropland were obtained (Table 3). The q-statistics of environmental factors from 2001 to 2020 ranged between 0.04 and 0.43, with an average value of 0.27. Among these factors, the highest explanatory power in 2005 was found for the mean annual temperature (MAT), with q-statistics of 0.46. The highest explanatory powers in 2010, 2015, and 2020 were found for the geomorphic type (GT), and the q-statistics values were 0.27, 0.22, and 0.22, respectively. The weakest explanatory power was observed for farming conditions (FC). These results lead us to infer that the geomorphological type and climatic characteristics are important determinants of the spatial distribution of abandoned cropland, whereas the effect of farming practice was relatively weak. The q-statistics values of socio-economic factors from 2001 to 2020 varied between 0.20 and 0.38, with a mean value of 0.31 (Table 3). Among these factors, the highest explanatory powers in 2005, 2010, and 2015 were found for GDP density (GDPD), with q-statistics values of 0.43, 0.29, and 0.15, respectively. The highest explanatory power in 2020 was found for population density (PD), with q-statistics of 0.12. Based on this, PD and GDP can significantly explain the pattern of cropland abandonment in Chongqing compared to road density (RD). Based on the q-statistics values from 2001 to 2020, the average contribution of socio-economic factors to cropland abandonment was 0.31, higher than that of the environmental factors (0.27).

Table 3. Values for q-statistics for the different factors and years.

Factors	q-Statistics				
	2005	2010	2015	2020	2001–2020
DEM	0.41	0.24	0.19	0.18	0.38
Slope	0.20	0.14	0.11	0.12	0.22
ST	0.28	0.16	0.11	0.12	0.26
GT	0.36	0.27	0.22	0.22	0.40
VT	0.22	0.13	0.09	0.07	0.20
FC	0.04	0.02	0.02	0.04	0.04
MATP	0.11	0.22	0.00	0.00	0.24
MAT	0.46	0.26	0.20	0.21	0.43
GDPD	0.43	0.29	0.15	0.11	0.38
PD	0.40	0.26	0.14	0.12	0.36
RD	0.27	0.15	0.05	0.10	0.20

The influence of the interaction between the independent variables on the dependent variables was also explored. Based on the results, the interactions between two independent variables exceeded those of individual variables (Figure 9). The interaction types were non-linear-enhanced and bi-enhanced. Among them, bi-enhanced was the main interaction type, indicating that the explanatory power of the interaction effect was stronger than that of a single factor. In 2015 and 2020, MATP and other factors showed a non-linear-enhanced effect, indicating that they exceeded the combined effects of their individual factors. Although the q-statistics values of the environmental factors were small, the interaction between the environmental factors and the other variables also had a strong impact on cropland abandonment. In terms of the time change, the interaction between most determinants showed a decreasing trend. Clearly, the most significant interaction effects occurred in 2005, when the effects of the MAT and GDPD interaction were most significant, with q-statistics of 0.56. In 2010 and 2015, the interaction between GDPD and GT had the greatest explanatory power, and the q-statistics values were 0.38 and 0.28, respectively. In 2020, the q-statistics of the interaction between MAT and MATP were highest, with a value of 0.28. Based on these results, the interaction between GDPD and

the other determinants was weakening. Generally, GDP, topographic factors, and climatic factors are the dominant interactive effects influencing cropland abandonment.
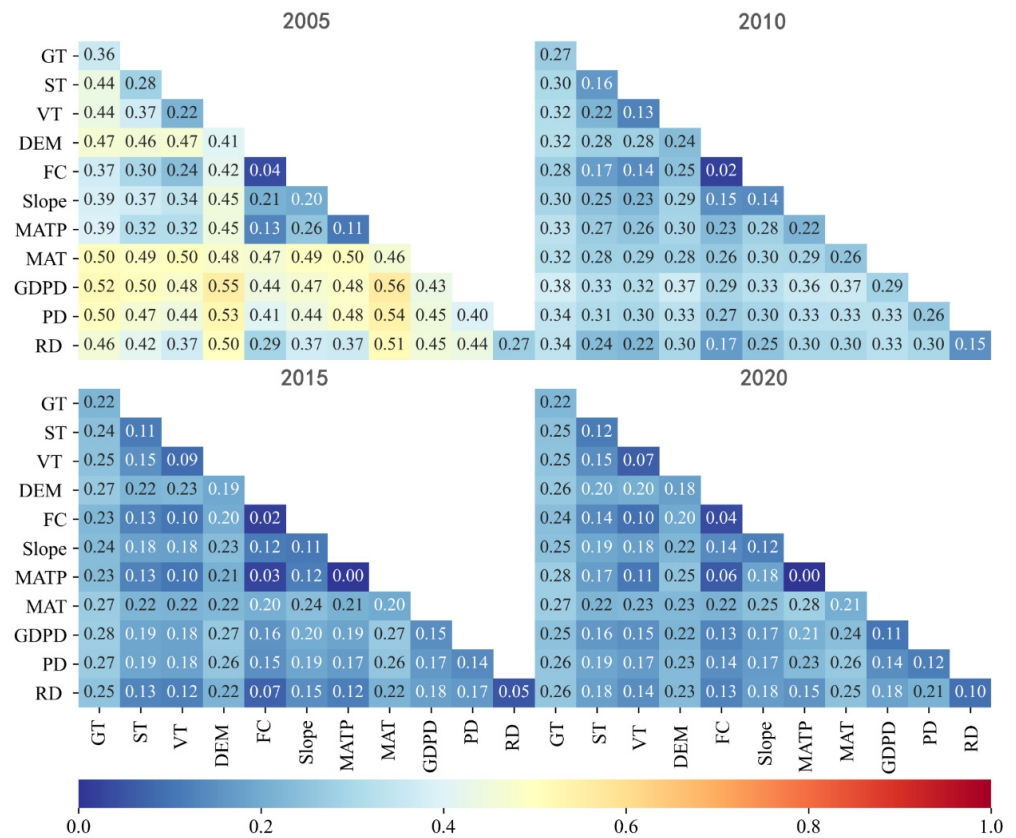
2005

	GT	ST	VT	DEM	FC	Slope	MATP	MAT	GDPD	PD	RD
GT	0.36										
ST	0.44	0.28									
VT	0.44	0.37	0.22								
DEM	0.47	0.46	0.47	0.41							
FC	0.37	0.30	0.24	0.42	0.04						
Slope	0.39	0.37	0.34	0.45	0.21	0.20					
MATP	0.39	0.32	0.32	0.45	0.13	0.26	0.11				
MAT	0.50	0.49	0.50	0.48	0.47	0.49	0.50	0.46			
GDPD	0.52	0.50	0.48	0.55	0.44	0.47	0.48	0.56	0.43		
PD	0.50	0.47	0.44	0.53	0.41	0.44	0.48	0.54	0.45	0.40	
RD	0.46	0.42	0.37	0.50	0.29	0.37	0.37	0.51	0.45	0.44	0.27

2010

	GT	ST	VT	DEM	FC	Slope	MATP	MAT	GDPD	PD	RD
GT	0.27										
ST	0.30	0.16									
VT	0.32	0.22	0.13								
DEM	0.32	0.28	0.28	0.24							
FC	0.28	0.17	0.14	0.25	0.02						
Slope	0.30	0.25	0.23	0.29	0.15	0.14					
MATP	0.33	0.27	0.26	0.30	0.23	0.28	0.22				
MAT	0.32	0.28	0.29	0.28	0.26	0.30	0.29	0.26			
GDPD	0.38	0.33	0.32	0.37	0.29	0.33	0.36	0.37	0.29		
PD	0.34	0.31	0.30	0.33	0.27	0.30	0.33	0.33	0.33	0.26	
RD	0.34	0.24	0.22	0.30	0.17	0.25	0.30	0.30	0.33	0.30	0.15

2015

	GT	ST	VT	DEM	FC	Slope	MATP	MAT	GDPD	PD	RD
GT	0.22										
ST	0.24	0.11									
VT	0.25	0.15	0.09								
DEM	0.27	0.22	0.23	0.19							
FC	0.23	0.13	0.10	0.20	0.02						
Slope	0.24	0.18	0.18	0.23	0.12	0.11					
MATP	0.23	0.13	0.10	0.21	0.03	0.12	0.00				
MAT	0.27	0.22	0.22	0.22	0.20	0.24	0.21	0.20			
GDPD	0.28	0.19	0.18	0.27	0.16	0.20	0.19	0.27	0.15		
PD	0.27	0.19	0.18	0.26	0.15	0.19	0.17	0.26	0.17	0.14	
RD	0.25	0.13	0.12	0.22	0.07	0.15	0.12	0.22	0.18	0.17	0.05

2020

	GT	ST	VT	DEM	FC	Slope	MATP	MAT	GDPD	PD	RD
GT	0.22										
ST	0.25	0.12									
VT	0.25	0.15	0.07								
DEM	0.26	0.20	0.20	0.18							
FC	0.24	0.14	0.10	0.20	0.04						
Slope	0.25	0.19	0.18	0.22	0.14	0.12					
MATP	0.28	0.17	0.11	0.25	0.06	0.18	0.00				
MAT	0.27	0.22	0.23	0.23	0.22	0.25	0.28	0.21			
GDPD	0.25	0.16	0.15	0.22	0.13	0.17	0.21	0.24	0.11		
PD	0.26	0.19	0.17	0.23	0.14	0.17	0.23	0.26	0.14	0.12	
RD	0.26	0.18	0.14	0.23	0.13	0.18	0.15	0.25	0.18	0.21	0.10

0.0　　　0.2　　　0.4　　　0.6　　　0.8　　　1.0

Figure 9. Interaction of factors affecting cropland abandonment.

5. Discussion

5.1. Estimation of Abandoned Cropland Area

The traditional methods to extract abandoned cropland are generally farmer surveys, interviews, questionnaires, etc. The greatest advantage of farmer surveys is that first-hand information can be obtained, enhancing our understanding of the causes of cropland abandonment from the perspective of farmers [51]. For example, by tracking farmer surveys from 2011 and 2018, Wang et al. [52] could determine that urbanization was the main factor influencing land marginalization, which increased labor costs and made agriculture unprofitable. However, the distribution of abandoned cropland could only be inferred and estimated through existing sample data, and it was difficult to determine continuous changes in the spatial distribution of abandoned cropland via investigation [6,53]. The methods of extracting abandoned cropland information based on remote sensing were mostly based on comparing the vegetation changes of the plots or the transfer of land use types [17,21]. For example, Shi et al. [54] extracted abandoned farmland parcels from farmland distribution maps, between 2002 and 2011, and calculated the abandonment rates for each township in three countries. This method required access to historical farmland data, and single-stage images could only determine the land use status during the time when the images were acquired. Due to the lack of process information on land use changes, even if the land use type was non-cultivated land at the time of image acquisition (unused land, grassland, etc.), it was difficult to determine whether the cropland had actually been abandoned or whether it was fallow or returned farmland. In this study, we derived a series of land use trajectories based on MODIS NDVI data and then used this information to assess the distribution of the abandoned cropland and the frequency of

cropland abandonment. More detailed information can be obtained, such as abandonment scope, time, and duration.

5.2. Cropland Abandonment Rate and Its Temporal Trend in Chongqing

The cropland abandonment map shows that about 13.3% of cropland within the study region was abandoned between 2001 and 2020, suggesting that cropland abandonment is widespread in Chongqing. Compared with other parts of the world, the values here were lower than those found for Chile (45.1% of cropland) [10], Poland and the Ukraine (20.7% and 13.9%) [11], and other mountainous areas of China, such as Guizhou Province (26%) [37], but slightly higher than those observed for Central Asia, where abandoned cropland accounts for 13% of the arable land area [40]. The overall cropland abandonment rate showed an initial increase, followed by a slight decrease, most likely as a result of the implementation of the "Grain for Green Program" (GGP), which was launched in 2002. The objectives of this program are to convert marginal farmland into forest land by compensating farmers for planting trees on retired farmland [55]. As the program comes to an end, the government will pay more attention to maintaining the stability of cropland and will reduce subsidies for long-term fallowed cropland, thereby reducing the direct benefits of farmers cultivating mountainous land with harsh environmental conditions. This will cause farmers to recultivate their land. In contrast, due to agricultural subsidies, farmers in other countries have abandoned cropland. For example, in the western and southern areas of Russia, due to the collapse of the former Soviet Union, the issuing of agricultural subsidies stopped, which resulted in widespread cropland abandonment [56].

5.3. Effects of Environmental and Socioeconomic Factors on Cropland Abandonment in Chongqing

According to a previous study, socio-economic development is an intrinsic factor affecting land use change [20]. The lack of labor and the aging of the agricultural labor force has a significant impact on cropland abandonment [20,57,58]. For example, cropland abandonment in the mountainous areas of Europe was considered to be closely related to the large migration of the rural population to the cities [59,60]. Although the total population has rapidly increased in the study area since 2001, with an accelerating GDP, the rural population generally declined. Urbanization and economic development lead to an increase in the employment transfer of rural labor, which potentially leads to a labor shortage and to increasing rural labor costs. This eventually leads to the marginalization and abandonment of cropland. The reform of the political system is also one of the reasons affecting cropland abandonment. For example, in eastern Europe and the former Soviet Union, land use intensity decreased significantly after the collapse of the USSR, and cropland abandonment and forest expansion became widespread [11,61,62]. In terms of the specific factors influencing cropland abandonment, previous studies showed that plots with poor soil quality, inconvenient transportation, and incomplete field infrastructure are more prone to abandonment [10,63–65]. However, the impact of natural factors on abandonment varies by region. For example, cropland abandonment in eastern Europe is mainly affected by location, whereas in western Europe, it is largely affected by land quality [63,65]. In Slovakia, the possibility of abandonment increases with the increasing distance from the capital, decreases with the increasing average annual temperature, and is generally higher near the forest edge and on steep slopes [66]. The geomorphological type and the climatic characteristics are the main environmental factors affecting cropland abandonment in the study area, which is consistent with the findings obtained elsewhere [25]. Unfavorable farming conditions and climate change reduce cropland yield and increase the cost of farming, thereby increasing the possibility of cropland marginalization [67].

5.4. Policy Impacts

The Chinese government proposed the "farmland red line" (at least 1.2 million km^2) to ensure national food security. China has experienced a rapid urbanization over the past few decades, but urban expansion has often increased at the expense of arable land, leading

to increasing pressure to maintain the red line. Moreover, low grain planting profits turned farmers to growing large numbers of fruit trees and other cash crops. The high costs of growing grain often exceed the benefits, whereas the income obtained from cash crops is often significantly higher [68]. To mitigate this issue, the Government must develop a series of agricultural policies, such as grain subsidies, to promote grain cultivation. The LFAs (Less Favored Areas) policy, implemented in Europe, seeks to improve the vulnerability of agriculture through subsidies. In mountainous areas of Europe, LFAs can help reduce the risk of cropland abandonment [6]. In addition, by increasing subsidies for the purchase of agricultural machinery, farmers can be encouraged to make full use of modern machinery to improve productivity and reduce costs. Furthermore, modern information technologies, such as satellite remote sensing, are required for the long-term monitoring and evaluation of cropland, and some countries have built remote sensing monitoring systems for agricultural conditions, such as the agriculture and resources inventory surveys through aerospace remote sensing (AgRISTARS) and Monitoring Agricultural ResourceS (MARS). The formulation of scientific planning measures needs to distinguish different land conditions and reasons for abandonment. For large areas of abandoned cropland with good geographical locations but an insufficient labor force, the government needs to establish a withdrawal mechanism for the land contract rights, especially for original farmers who have settled in cities. In the case of scattered cropland distribution, the promotion of concentrated cropland areas and the rebuilding of land production units are crucial to mitigate cropland fragmentation. Spatially, China's abandoned cropland is mostly concentrated in mountainous areas, such as Chongqing. Yield-increasing technologies can be used to increase the intensification of high-quality arable land while, at the same time, reducing the dependence on mountainous cropland and promoting the restoration of forest vegetation on marginal lands [69].

6. Conclusions

In this study, the MODIS NDVI time series and phenological parameters were used to obtain the land use trajectory of each pixel. Subsequently, the extent and spatial patterns of abandoned cropland were mapped using a set threshold length of farming cessation. From 2001 to 2020, the cropland abandonment rate ranged from 12.2 to 15.4%, with an average of 13.3% (4185.2 km^2). This rate initially increased and then decreased. There was a large spatial difference in the distribution of abandoned farmland, and the overall distribution pattern showed a gradually increasing trend from the southwest to the north and southeast. Moreover, the spatial distribution of abandoned cropland was clearly clustered, with high-value areas being concentrated in the north and southeast and low-value areas in the southwest.

The spatial distribution of abandoned cropland was mainly influenced by socioeconomic factors, following the order GDPD, PD, and RD. Based on the q-statistics from 2001 to 2020, the average contribution of socio-economic factors to cropland abandonment is greater than that of the environmental factors. The q-statistics followed the order MAT, GT, DEM, ST, MATP, Slope, VT, and FC. The two-factor interaction is mainly manifested as bi-enhanced, with a lower nonlinear enhancement effect. The interaction between the two factors exceeds the effect of a single factor.

The findings obtained in this study can serve as a basis for the development of adequate policies to control cropland abandonment, such as providing grain subsidies, undertaking cropland consolidation, encouraging land transfer, and improving agricultural infrastructure, while reducing the dependence on mountainous cropland and promoting the restoration of forest vegetation on marginal lands. Modern information technologies are required for the long-term monitoring and evaluation of cropland.

Institutional Review Board Statement: Not applicable.

Informed Consent Statement: Not applicable.

Data Availability Statement: All relevant data sets in this study are described in the manuscript.

Conflicts of Interest: The authors declare no conflict of interest.

Appendix A

Appendix A.1 The Specific Process of Generating the Annual Land Use Maps

(1) Reconstructed NDVI Time Series:

The discrimination accuracy of cultivated land and abandoned areas in low-resolution remote sensing images can be effectively improved by using NDVI time series and the corresponding phenological characteristics of the growth period [41]. The NDVI values of each pixel were first arranged in chronological order from 2001 to 2020, with each time series comprising a total of 460 values. The NDVI time series may be affected by background noise caused by atmospheric changes, snow, and clouds, leading to inaccurate NDVI values. The NDVI smoothing time series was reconstructed with a Savitzky-Golay filter for noise reduction, using the TIMESAT3.3 tool. Subsequently, the NDVI smoothed time series were processed to obtain 13 annual phenological indicators for each pixel [42]. These metrics were season length, mid-season time, maximum value, base value, amplitude, small integrated values, large integrated values, start and end of the season value, as well as the beginning and end of a season.

(2) Selecting Training and Validation Samples:

The training and validation samples were selected according to the land use data, including MCD12Q1, ESA, LUCC, and GlobeLand30. First, land use types were divided into cropland, forest, grassland, water, built-up areas, and unused land. All land use data were projected into the same Albers_WGS_1984 coordinate system and then masked to the same spatial boundary with the study area. Subsequently, the spatial resolution was unified to 250 m using the resampling method. A series of steps were used to select and label the yearly samples. Specifically, through image stacking processing of land use data, the pixels that remained stable from 2001 to 2020 in different land use data were selected, and the stable pixels of each land use type were collected to generate a sample database. This method was used to reduce sample uncertainty and improve sample selection accuracy. After that, in the sample database, a stratified random sampling method was adopted to select training samples for each land use type, and finally, about 10,000 training samples were obtained each year. In the remaining sample database, approximately 2000 independent random points were selected as verification samples for each year.

(3) Land Use Classification:

We applied the random forest classification for mapping the annual land use type. The classifier was composed of multiple decision tree models and worked effectively in land cover classification [43]. Overall, 36 features were imported for each year for the random forest classification, including 23 smooth NDVI values and 13 phenological indices collected in each growing season from 2001 to 2020. The random forest models used in this analysis were simulated using the Scikit-learn machine learning library in Python and, subsequently, the land use map for each year (from 2001–2020) was generated.

Appendix A.2 Specific Calculation Procedure of the q-Statistics Values

The calculation method is as follows [49]:

$$q = 1 - \frac{\sum_{h=1}^{L} N_h \delta_h^2}{N \delta^2},$$

(A1)

where "q" is the explanatory power of the influence factor on the cropland abandonment rate, "N" is the sample size, "L" is the classification number of the index factors, and "N_h" and "δ_h^2" represent the variances of the sample size in layer "h" and the cropland abandonment rate, respectively. The value of the q-statistics was in the range of (0,1). The larger the value, the stronger the explanatory power of the influencing factor on cropland abandonment, and its spatial distribution is consistent with the cropland abandonment rate. When the q-statistics are equal to 0, the given impact factor has no significant relationship with the cropland abandonment situation. At a value of 1, the impact factor can fully explain the spatial variation in abandoned cropland.
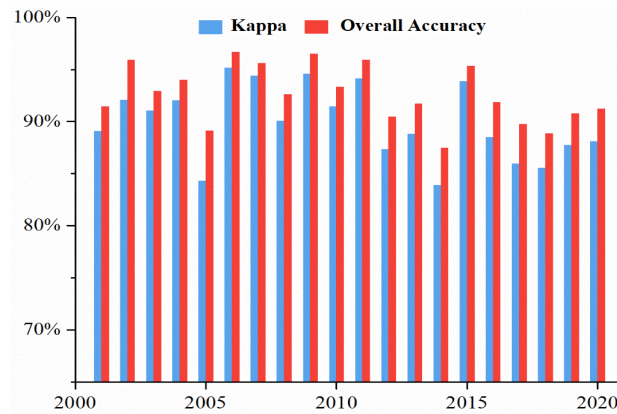
Figure A1. Annual land use classification accuracy.
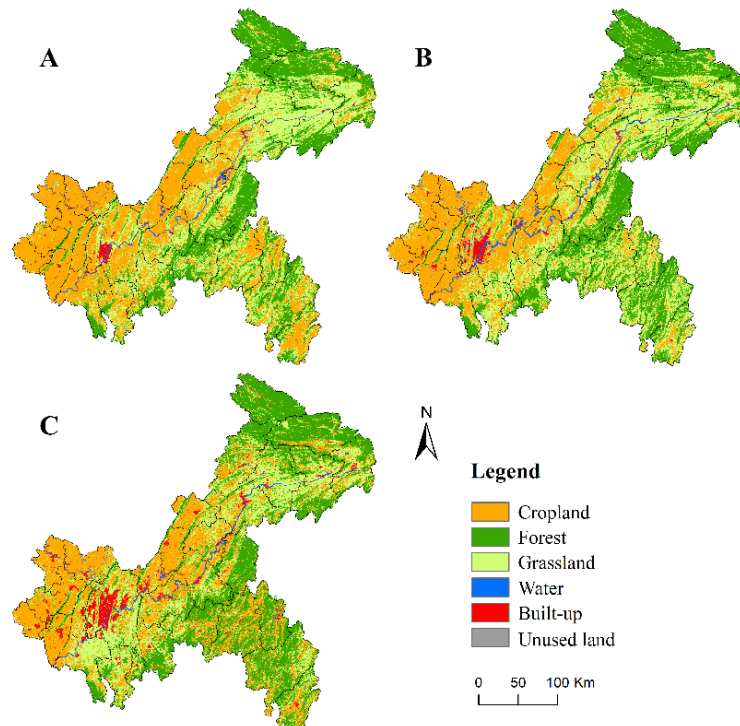
Figure A2. Land use map of Chongqing for (**A**) 2001, (**B**) 2010, and (**C**) 2020.
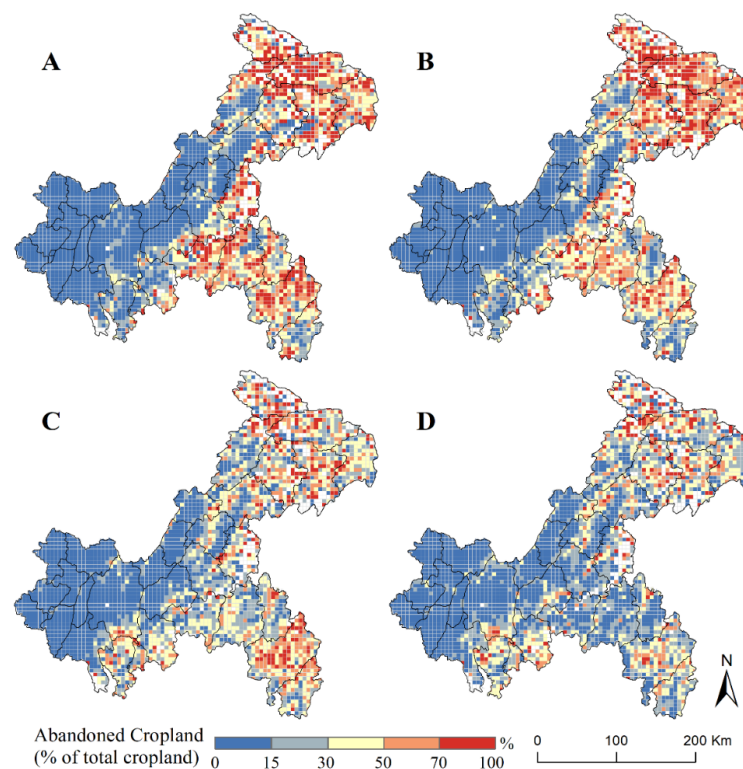
Figure A3. Average cropland abandonment rates within 5 km grid squares in Chongqing for (**A**) 2001–2005, (**B**) 2006–2010, (**C**) 2011–2015, (**D**), and 2016–2020.

References

1. Godfray, H.C.J.; Beddington, J.R.; Crute, I.R.; Haddad, L.; Lawrence, D.; Muir, J.F.; Pretty, J.; Robinson, S.; Thomas, S.M.; Toulmin, C. Food Security: The Challenge of Feeding 9 Billion People. *Science* **2010**, *327*, 812–818. [CrossRef]
2. Ash, C.; Jasny, B.R.; Malakoff, D.A.; Sugden, A.M. Feeding the Future. *Science* **2010**, *327*, 797. [CrossRef] [PubMed]
3. West, P.C.; Gerber, J.S.; Engstrom, P.M.; Mueller, N.D.; Brauman, K.A.; Carlson, K.M.; Cassidy, E.S.; Johnston, M.; MacDonald, G.K.; Ray, D.K.; et al. Leverage points for improving global food security and the environment. *Science* **2014**, *345*, 325–328. [CrossRef] [PubMed]
4. Chen, G.; Li, X.; Liu, X.; Chen, Y.; Liang, X.; Leng, J.; Xu, X.; Liao, W.; Qiu, Y.; Wu, Q.; et al. Global projections of future urban land expansion under shared socioeconomic pathways. *Nat. Commun.* **2020**, *11*, 537. [CrossRef] [PubMed]
5. Zhou, Y. Report on China's development and investment in land and water. *FAO Investig. Land Water Bangk.* **2002**, *09*, 187–207.
6. Li, S.; Li, X. Global understanding of farmland abandonment: A review and prospects. *J. Geogr. Sci.* **2017**, *27*, 1123–1150. [CrossRef]
7. Queiroz, C.; Beilin, R.; Folke, C.; Lindborg, R. Farmland abandonment: Threat or opportunity for biodiversity conservation? A global review. *Front. Ecol. Environ.* **2014**, *12*, 288–296. [CrossRef]
8. Hatna, E.; Bakker, M.M. Abandonment and Expansion of Arable Land in Europe. *Ecosystems* **2011**, *14*, 720–731. [CrossRef]
9. Keenleyside, C.; Tucker, G. *Farmland Abandonment in the EU: An Assessment of Trends and Prospects. Report Prepared for WWF*; Institute for European Environmental Policy Press: London, UK, 2010.
10. Díaz, G.I.; Nahuelhual, L.; Echeverría, C.; Marín, S. Drivers of land abandonment in Southern Chile and implications for landscape planning. *Landsc. Urban Plan* **2011**, *99*, 207–217. [CrossRef]
11. Kuemmerle, T.; Olofsson, P.; Chaskovskyy, O.; Baumann, M.; Ostapowicz, K.; Woodcock, C.E.; Houghton, R.A.; Hostert, P.; Keeton, W.S.; Radeloff, V.C. Post-Soviet farmland abandonment, forest recovery, and carbon sequestration in western Ukraine. *Glob. Chang. Biol.* **2011**, *17*, 1335–1349. [CrossRef]
12. Li, S.; Li, X.; Xin, L.; Tan, M.; Wang, X.; Wang, R.; Jiang, M.; Wang, Y. Extent and distribution of cropland abandonment in Chinese mountainous areas. *Resour. Sci.* **2017**, *39*, 1801–1811. [CrossRef]
13. Yin, H.; Prishchepov, A.V.; Kuemmerle, T.; Bleyhl, B.; Buchner, J.; Radeloff, V.C. Mapping agricultural land abandonment from spatial and temporal segmentation of Landsat time series. *Remote Sens. Environ.* **2018**, *210*, 12–24. [CrossRef]
14. Morell-Monzo, S.; Estornell, J.; Sebastia-Frasquet, M.-T. Comparison of Sentinel-2 and High-Resolution Imagery for Mapping Land Abandonment in Fragmented Areas. *Remote Sens.* **2020**, *12*, 2062. [CrossRef]

15. Paudel, B.; Wu, X.; Zhang, Y.; Rai, R.; Liu, L.; Zhang, B.; Khanal, N.R.; Koirala, H.L.; Nepal, P. Farmland abandonment and its determinants in the different ecological villages of the Koshi river basin, central Himalayas: Synergy of high-resolution remote sensing and social surveys. *Environ. Res.* **2020**, *188*, 109711. [CrossRef]

16. Goga, T.; Feranec, J.; Bucha, T.; Rusnak, M.; Sackov, I.; Barka, I.; Kopecka, M.; Papco, J.; Otahel, J.; Szatmari, D.; et al. A Review of the Application of Remote Sensing Data for Abandoned Agricultural Land Identification with Focus on Central and Eastern Europe. *Remote Sens.* **2019**, *11*, 2759. [CrossRef]

17. Skakun, S.V.; Justice, C.O.; Kussul, N.; Shelestov, A.; Lavreniuk, M. Satellite Data Reveal Cropland Losses in South-Eastern Ukraine Under Military Conflict. *Front. Earth Sci.* **2019**, *7*, 305. [CrossRef]

18. Wang, L.; Zhou, Z.; Zhao, X.; Kong, J.; Zhang, S. Spatiotemporal Evolution of Karst Rocky Desertification Abandoned Cropland Based on Farmland-parcels Time-series Remote Sensing. *J. Soil Water Conserv.* **2020**, *34*, 92–99. [CrossRef]

19. Alcantara, C.; Kuemmerle, T.; Baumann, M.; Bragina, E.V.; Griffiths, P.; Hostert, P.; Knorn, J.; Mueller, D.; Prishchepov, A.V.; Schierhorn, F.; et al. Mapping the extent of abandoned farmland in Central and Eastern Europe using MODIS time series satellite data. *Environ. Res. Lett.* **2013**, *8*, 035035. [CrossRef]

20. Prishchepov, A.V.; Müller, D.; Dubinin, M.; Baumann, M.; Radeloff, V.C. Determinants of agricultural land abandonment in post-Soviet European Russia. *Land Use Policy* **2013**, *30*, 873–884. [CrossRef]

21. Yusoff, N.M.; Muharam, F.M.; Khairunniza-Bejo, S. Towards the use of remote-sensing data for monitoring of abandoned oil palm lands in Malaysia: A semi-automatic approach. *Int. J. Remote Sens.* **2017**, *38*, 432–449. [CrossRef]

22. Alonso-Sarría, F.; Martínez-Hernández, C.; Romero-Díaz, A.; Cánovas-García, F.; Gomariz-Castillo, F. Main Environmental Features Leading to Recent Land Abandonment in Murcia Region (Southeast Spain). *Land Degrad. Dev.* **2016**, *27*, 654–670. [CrossRef]

23. Ustaoglu, E.; Collier, M.J. Farmland abandonment in Europe: An overview of drivers, consequences, and assessment of the sustainability implications. *Environ. Rev.* **2018**, *26*, 396–416. [CrossRef]

24. Hinojosa, L.; Napoléone, C.; Moulery, M.; Lambin, E.F. The "mountain effect" in the abandonment of grasslands: Insights from the French Southern Alps. *Agric. Ecosyst. Environ.* **2016**, *221*, 115–124. [CrossRef]

25. Benayas, J.; Martins, A.; Nicolau, J.; Schulz, J.J. Abandonment of agricultural land: An overview of drivers and consequences. CAB Reviews: Perspectives in Agriculture, Veterinary Science. *Nutr. Nat. Resour.* **2007**, *2*, 1–14.

26. Lambin, E.F.; Meyfroidt, P. Global land use change, economic globalization, and the looming land scarcity. *Proc. Natl. Acad. Sci. USA* **2011**, *108*, 3465. [CrossRef]

27. Zhang, Y.; Li, X.; Song, W.; Shi, T. Effect of agricultural laborer on cropland abandonment under land circulation at different levels in Wulong County, Chongqing City. *Prog. Phys. Geogr.* **2014**, *33*, 552–560. [CrossRef]

28. Yan, J.; Zhuo, R.; Xie, D.; Zhang, Y. Land Use Characters of Farmers of Different Livelihood Strategies: Cases in Three Gorges Reservoir Area. *Acta Geogr. Sin.* **2010**, *65*, 1401–1410. [CrossRef]

29. United States Geological Survey. Available online: https://lpdaac.usgs.gov (accessed on 10 March 2021).

30. Friedl, M.A.; Sulla-Menashe, D.; Tan, B.; Schneider, A.; Ramankutty, N.; Sibley, A.; Huang, X. MODIS Collection 5 global land cover: Algorithm refinements and characterization of new datasets. *Remote Sens. Environ.* **2010**, *114*, 168–182. [CrossRef]

31. European Space Agency. Available online: http://www.esa-landcover-cci.org (accessed on 10 March 2021).

32. Liu, J.; Kuang, W.; Zhang, Z.; Xu, X.; Qin, Y.; Ning, J.; Zhou, W.; Zhang, S.; Li, R.; Yan, C.; et al. Spatiotemporal characteristics, patterns, and causes of land-use changes in China since the late 1980s. *J. Geogr. Sci.* **2014**, *24*, 195–210. [CrossRef]

33. Resource Environmental Science and Data Center, Chinese Academy of Sciences. Available online: http://www.resdc.cn/Default.aspx (accessed on 5 March 2021).

34. National Geomatics Center of China. Available online: http://www.globallandcover.com (accessed on 10 March 2021).

35. National Meteorological Science Data Center. Available online: http://data.cma.cn/ (accessed on 10 March 2021).

36. Chongqing Statistics Bureau. Available online: http://tjj.cq.gov.cn (accessed on 10 March 2021).

37. Li, S.; Li, X.; Sun, L.; Cao, G.; Fischer, G.; Tramberend, S. An estimation of the extent of cropland abandonment in mountainous regions of China. *Land Degrad. Dev.* **2018**, *29*, 1327–1342. [CrossRef]

38. Löw, F.; Fliemann, E.; Abdullaev, I.; Conrad, C.; Lamers, J.P.A. Mapping abandoned agricultural land in Kyzyl-Orda, Kazakhstan using satellite remote sensing. *Appl. Geogr.* **2015**, *62*, 377–390. [CrossRef]

39. Su, G.; Okahashi, H.; Chen, L. Spatial Pattern of Farmland Abandonment in Japan: Identification and Determinants. *Sustainability* **2018**, *10*, 3676. [CrossRef]

40. Low, F.; Prishchepov, A.V.; Waldner, F.; Dubovyk, O.; Akramkhanov, A.; Biradar, C.; Lamers, J.P.A. Mapping Cropland Abandonment in the Aral Sea Basin with MODIS Time Series. *Remote Sens.* **2018**, *10*, 159. [CrossRef]

41. Congalton, R.G. A review of assessing the accuracy of classifications of remotely sensed data. *Remote Sens. Environ.* **1991**, *37*, 35–46. [CrossRef]

42. Haining, R. *Spatial Data Analysis in the Social and Environmental Sciences*; Cambridge University Press: Cambridge, UK, 1993.

43. Anselin, L. *Spatial econometrics: Methods and models*; Kluwer Academic Press: Norwell, MA, USA, 1988.

44. Moran, P.A. The interpretation of statistical maps. *J. R. Stat. Soc.* **1948**, *10*, 243–251. [CrossRef]

45. Anselin, L. Local Indicators of Spatial Association—LISA. *Geogr. Anal.* **1995**, *27*, 93–115. [CrossRef]

46. Ord, J.K.; Getis, A. Local Spatial Autocorrelation Statistics: Distributional Issues and an Application. *Geogr. Anal.* **1995**, *27*, 286–306. [CrossRef]

47. Mann, H.B. Nonparametric Tests Against Trend. *Econometrica* **1945**, *13*, 245–259. [CrossRef]

48. Emerging Hot Spot Analysis. Available online: https://pro.arcgis.com/en/pro-app/latest/tool-reference/space-time-pattern-mining/emerginghotspots.htm (accessed on 20 March 2021).

49. Wang, J.; Xu, C. Geodetector: Principle and prospective. *Acta Geogr. Sin.* **2017**, *72*, 116–134. [CrossRef]

50. Han, Z.; Song, W. Abandoned cropland: Patterns and determinants within the Guangxi Karst Mountainous Area, China. *Appl. Geogr.* **2020**, *122*, 102245. [CrossRef]

51. Zhang, Y.; Li, X.; Zhai, L. Land abandonment under rural restructuring in China explained from a cost-benefit perspective. *J. Rural. Stud.* **2016**, *47*, 524–532. [CrossRef]

52. Wang, Y.; Li, X.; Xin, L.; Tan, M. Farmland marginalization and its drivers in mountainous areas of China. *Sci. Total Environ.* **2020**, *719*, 135132. [CrossRef] [PubMed]

53. Zhang, Y.; Li, X.; Song, W. Determinants of cropland abandonment at the parcel, household and village levels in mountain areas of China: A multi-level analysis. *Land Use Policy* **2014**, *41*, 186–192. [CrossRef]

54. Shi, T.; Li, X.; Xin, L.; Xu, X. The spatial distribution of farmland abandonment and its influential factors at the township level: A case study in the mountainous area of China. *Land Use Policy* **2018**, *70*, 510–520. [CrossRef]

55. Zhang, Z.; Zinda, J.A.; Li, W. Forest transitions in Chinese villages: Explaining community-level variation under the returning forest to farmland program. *Land Use Policy* **2017**, *64*, 245–257. [CrossRef]

56. Hölzel, N.; Haub, C.; Ingelfinger, M.P.; Otte, A.; Pilipenko, V.N. The return of the steppe large-scale restoration of degraded land in southern Russia during the post-Soviet era. *J. Nat. Conserv.* **2002**, *10*, 75–85. [CrossRef]

57. Pinto-Correia, T. Land abandonment: Changes in the land use patterns around the Mediterranean basin. *Cah. Options Méditerr.* **1993**, *1*, 97–112.

58. Melendez-Pastor, I.; Hernandez, E.I.; Navarro-Pedreno, J.; Gomez, I. Socioeconomic factors influencing land cover changes in rural areas: The case of the Sierra de Albarracin (Spain). *Appl. Geogr.* **2014**, *52*, 34–45. [CrossRef]

59. Jokisch, B.D. Migration and Agricultural Change: The Case of Smallholder Agriculture in Highland Ecuador. *Hum. Ecol.* **2002**, *30*, 523–550. [CrossRef]

60. Vacquie, L.A.; Houet, T.; Sohl, T.L.; Reker, R.; Sayler, K.L. Modelling regional land change scenarios to assess land abandonment and reforestation dynamics in the Pyrenees (France). *J. Mt. Sci.* **2015**, *12*, 905–920. [CrossRef]

61. Schierhorn, F.; Mueller, D.; Beringer, T.; Prishchepov, A.V.; Kuemmerle, T.; Balmann, A. Post-Soviet cropland abandonment and carbon sequestration in European Russia, Ukraine, and Belarus. *Glob. Biogeochem. Cycles* **2013**, *27*, 1175–1185. [CrossRef]

62. Ho, N.; Hoelzel, N.; Voelker, A.; Kamp, J. Patterns and Determinants of Post-Soviet Cropland Abandonment in the Western Siberian Grain Belt. *Remote Sens.* **2018**, *10*, 1973. [CrossRef]

63. Xie, H.; Wang, P.; Yao, G. Exploring the Dynamic Mechanisms of Farmland Abandonment Based on a Spatially Explicit Economic Model for Environmental Sustainability: A Case Study in Jiangxi Province, China. *Sustainability* **2014**, *6*, 1260–1282. [CrossRef]

64. Kerckhof, A.; Spalevic, V.; Van Eetvelde, V.; Nyssen, J. Factors of land abandonment in mountainous Mediterranean areas: The case of Montenegrin settlements. *Springerplus* **2016**, *5*, 485. [CrossRef]

65. Van Dijk, G.; Zdanowicz, A.; Blokzijl, R. *Land abandonment, biodiversity and the CAP*; DLG Service for Land and Water Management Press: Utrecht, The Netherlands, 2005.

66. Pazur, R.; Lieskovsky, J.; Buergi, M.; Mueller, D.; Lieskovsky, T.; Zhang, Z.; Prischchepov, A.V. Abandonment and Recultivation of Agricultural Lands in Slovakia-Patterns and Determinants from the Past to the Future. *Land* **2020**, *9*, 316. [CrossRef]

67. Yan, J.; Yang, Z.; Li, Z.; Li, X.; Xin, L.; Sun, L. Drivers of cropland abandonment in mountainous areas: A household decision model on farming scale in Southwest China. *Land Use Policy* **2016**, *57*, 459–469. [CrossRef]

68. National Development and Reform Commission (NDRC). *National Cost—Income Data of Agricultural Product*; China Statistics Press: Beijing, China, 2019.

69. Tachibana, T.; Nguyen, T.M.; Otsuka, K. Agricultural Intensification versus Extensification: A Case Study of Deforestation in the Northern-Hill Region of Vietnam. *J. Environ. Econ. Manag.* **2001**, *41*, 44–69. [CrossRef]